Electronic Supplementary Information (ESI)

Lanthanide dinuclear complexes constructed from mixed oxygen-donor ligands: effect of substituent positions of the neutral ligand on the magnetic dynamics in the Dy analogues

Wen-Hua Zhu,*[a] Shan Li,[a] Chen Gao,[b] Xia Xiong,[a] Yan Zhang,[a] Li Liu,[a] Annie K Powell,[c] and Song Gao*[b]

[a] *Hubei Collaborative Innovation Center for Advanced Organic Chemical Materials, Ministry-of-Education Key Laboratory for the Synthesis and Application of Organic Functional Molecules, College of Chemistry and Chemical Engineering, Hubei University, Wuhan 430062, PR China.*

[b] *Beijing National Laboratory for Molecular Sciences, State Key Laboratory of Rare Earth Materials Chemistry and Applications, College of Chemistry and Molecular Engineering, Peking University, No. 5 Yiheyuan Road, Beijing 100871, China.*

[c] *Institute of Inorganic Chemistry, Karlsruhe Institute of Technology, Engesserstrasse 15, Karlsruhe 76131, Germany.*

Electronic Supplementary Materials (ESI) for Daton Transactions

Table S1 Selected bond lengths (Å) and angles (°) for **1**

Dy(1)–O(1)	2.278(2)	Dy(1)–O(2)#1	2.322(2)
Dy(1)–O(3)	2.291(2)	Dy(1)–O(4)	2.432(2)
Dy(1)–O(5)	2.414(2)	Dy(1)–O(6)	2.454(2)
Dy(1)–O(7)	2.405(2)	Dy(1)–O(8)	2.383(2)
O(1)–Dy(1)–O(2)#1	111.52(8)	O(1)–Dy(1)–O(3)	151.74(9)
O(1)–Dy(1)–O(4)	82.96(8)	O(1)–Dy(1)–O(5)	86.69(8)
O(1)–Dy(1)–O(6)	125.32(8)	O(1)–Dy(1)–O(7)	74.37(8)
O(1)–Dy(1)–O(8)	76.60(8)	O(2)#1–Dy(1)–O(3)	81.53(8)
O(2)#1–Dy(1)–O(4)	146.72(8)	O(2)#1–Dy(1)–O(5)	151.39(9)
O(2)#1–Dy(1)–O(6)	76.63(9)	O(2)#1–Dy(1)–O(7)	78.42(9)
O(2)#1–Dy(1)–O(8)	77.51(9)	O(3)–Dy(1)–O(4)	74.04(8)
O(3)–Dy(1)–O(5)	92.53(9)	O(3)–Dy(1)–O(6)	81.31(9)
O(3)–Dy(1)–O(7)	133.80(8)	O(3)–Dy(1)–O(8)	82.37(9)
O(4)–Dy(1)–O(5)	53.64(8)	O(4)–Dy(1)–O(6)	120.39(8)
O(4)–Dy(1)–O(7)	134.85(7)	O(4)–Dy(1)–O(8)	77.15(8)
O(5)–Dy(1)–O(6)	74.81(9)	O(5)–Dy(1)–O(7)	86.05(8)
O(5)–Dy(1)–O(8)	129.68(9)	O(6)–Dy(1)–O(7)	53.76(8)
O(6)–Dy(1)–O(8)	151.11(9)	O(7)–Dy(1)–O(8)	131.74(8)

Symmetry codes： #1 –x, –y, –z

Table S2 Hydrogen bonding geometry for **1**: lengths (Å) and angles (°)

D–H···A	d(D–H)	d(H···A)	d(D···A)	<(DHA)
O(8)–H(81)···O(7)#1	0.946(17)	1.811(18)	2.752(3)	172(4)
O(8)–H(82)···O(4)#2	0.915(18)	1.857(19)	2.765(3)	172(4)

Symmetry codes： #1 –x, –y, –z，#2 –x+1, –y, –z

Table S3 Selected bond lengths (Å) and angles (°) for **7**

Dy(1)–O(1)	2.289(2)	Dy(1)–O(2)#1	2.348(2)
Dy(1)–O(3)	2.282(2)	Dy(1)–O(4)	2.434(2)
Dy(1)–O(5)	2.431(2)	Dy(1)–O(6)	2.486(2)
Dy(1)–O(7)	2.388(2)	Dy(1)–O(8)	2.363(2)
O(1)–Dy(1)–O(2)#1	113.50(8)	O(1)–Dy(1)–O(3)	151.71(8)
O(1)–Dy(1)–O(4)	83.55(7)	O(1)–Dy(1)–O(5)	88.26(8)
O(1)–Dy(1)–O(6)	125.33(7)	O(1)–Dy(1)–O(7)	74.90(7)
O(1)–Dy(1)–O(8)	76.47(8)	O(2)#1–Dy(1)–O(3)	79.69(8)
O(2)#1–Dy(1)–O(4)	143.52(7)	O(2)#1–Dy(1)–O(5)	150.86(8)
O(2)#1–Dy(1)–O(6)	76.74(8)	O(2)#1–Dy(1)–O(7)	80.36(8)
O(2)#1–Dy(1)–O(8)	77.75(8)	O(3)–Dy(1)–O(4)	72.81(8)
O(3)–Dy(1)–O(5)	89.96(8)	O(3)–Dy(1)–O(6)	81.11(8)
O(3)–Dy(1)–O(7)	133.22(8)	O(3)–Dy(1)–O(8)	82.59(8)
O(4)–Dy(1)–O(5)	53.62(7)	O(4)–Dy(1)–O(6)	120.80(7)
O(4)–Dy(1)–O(7)	136.11(7)	O(4)–Dy(1)–O(8)	75.39(8)
O(5)–Dy(1)–O(6)	74.77(7)	O(5)–Dy(1)–O(7)	87.46(8)
O(5)–Dy(1)–O(8)	128.18(8)	O(6)–Dy(1)–O(7)	53.22(7)
O(6)–Dy(1)–O(8)	151.76(9)	O(7)–Dy(1)–O(8)	132.84(8)

Symmetry codes： #1 –x, –y, –z

Table S4 Hydrogen bonding geometry for **7**: lengths (Å) and angles (°)

D–H···A	d(D–H)	d(H···A)	d(D···A)	<(DHA)
O(8)–H(81)···O(7)#1	0.932(18)	1.83(2)	2.728(3)	161(4)
O(8)–H(82)···O(4)#2	0.921(18)	1.823(19)	2.738(3)	172(4)

Symmetry codes： #1 –x, –y, –z，#2 –x+1, –y, –z

Table S5 Continuous shaped measures (CShM) for **1** and **7** using SHAPE 2.1

	1	**7**
OP-8	31.032	31.183
HPY-8	21.202	21.406
HBPY-8	12.656	12.542
CU-8	9.451	9.242
SAPR-8	2.796	3.115
TDD-8	3.056	3.399
JGBF-8	12.200	11.968
JETBPY-8	26.314	25.954
JBTPR-8	2.899	2.878
BTPR-8	2.196	2.192
JSD-8	4.078	4.323
TT-8	10.294	9.959

OP-8 = (D_{8h}) Octagon
HPY-8 = (C_{7v}) Heptagonal pyramid
HBPY-8 = (D_{6h}) Hexagonal bipyramid
CU-8 = (O_h) Cube
SAPR-8 = (D_{4d}) Square antiprism
TDD-8 = (D_{2d}) Triangular dodecahedron
JGBF-8 = (D_{2d}) Johnson gyrobifastigium J26
JETBPY-8 = (D_{3h}) Johnson elongated triangular bipyramid J14
JBTPR-8 = (C_{2v}) Biaugmented trigonal prism J50
BTPR-8 = (C_{2v}) Biaugmented trigonal prism
JSD-8 = (D_{2d}) Snub diphenoid J84
TT-8 = (T_d) Triakis tetrahedron

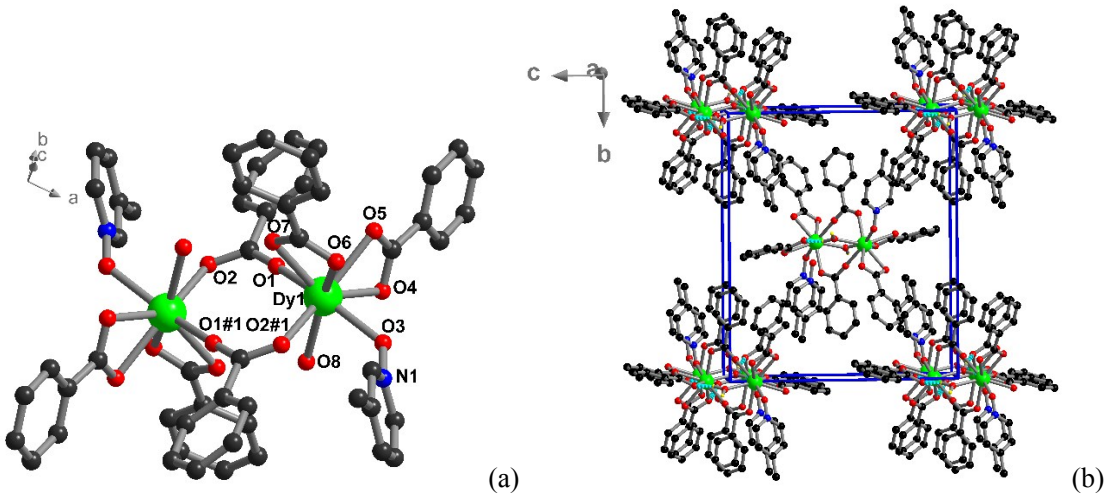

Fig. S1 (a) View of the dinuclear structure bridged by Bza ligands in complex **1**. (b) View of the packing diagram of complex **7** along the *a*-axis.

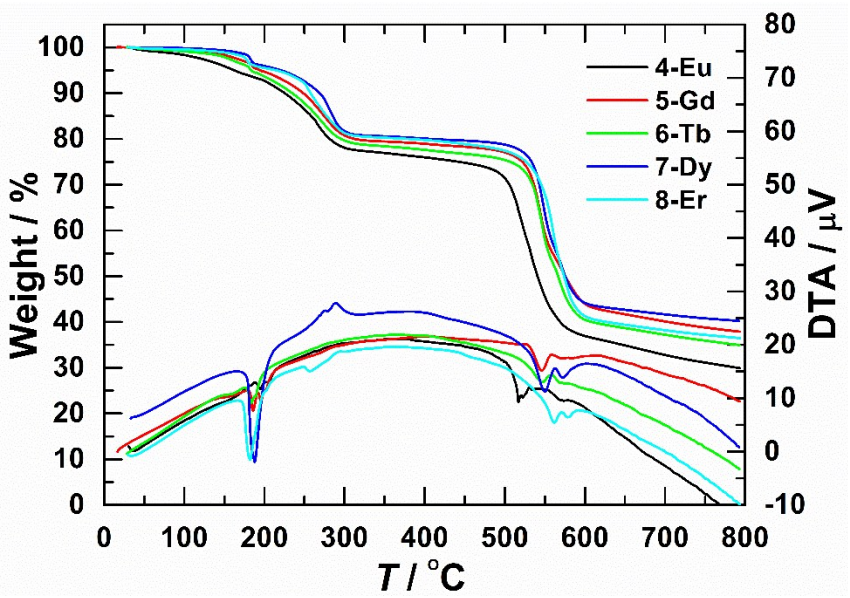

Fig. S2 The TG–DTA curves for complexes **4–8**.

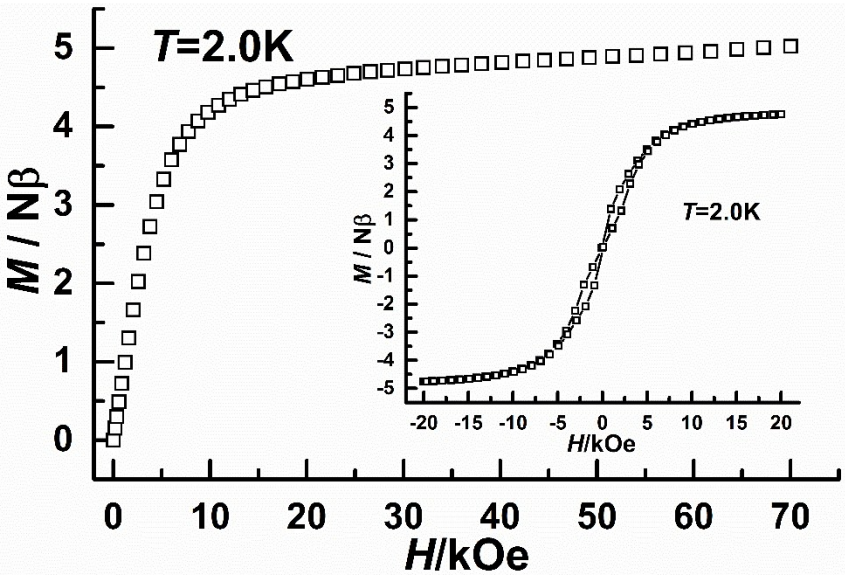

Fig. S3 Field dependence of the magnetization of compound **1** at 2.0 K. Inset: the hysteresis loop plot of compound **1** measured at 2.0 K.

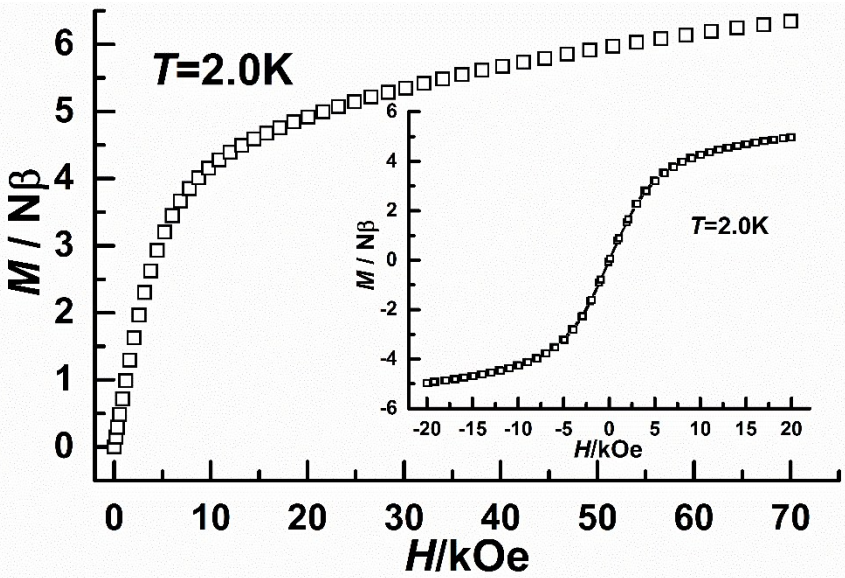

Fig. S4 Field dependence of the magnetization of compound **7** at 2.0 K. Inset: the hysteresis loop plot of compound **7** measured at 2.0 K.

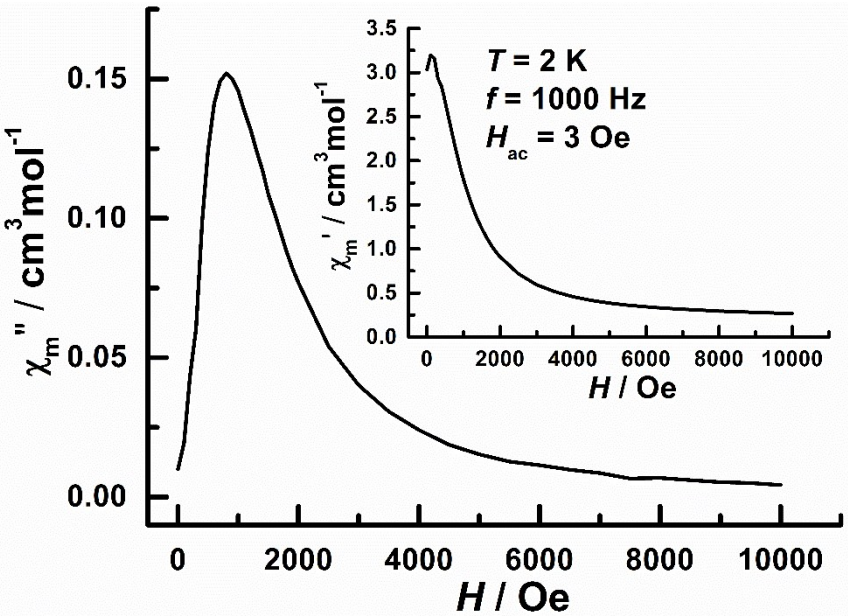

Fig. S5 Field dependence of the in-phase (χ', inset) and out-of-phase (χ'') ac susceptibility for **1** with f = 1000 Hz.

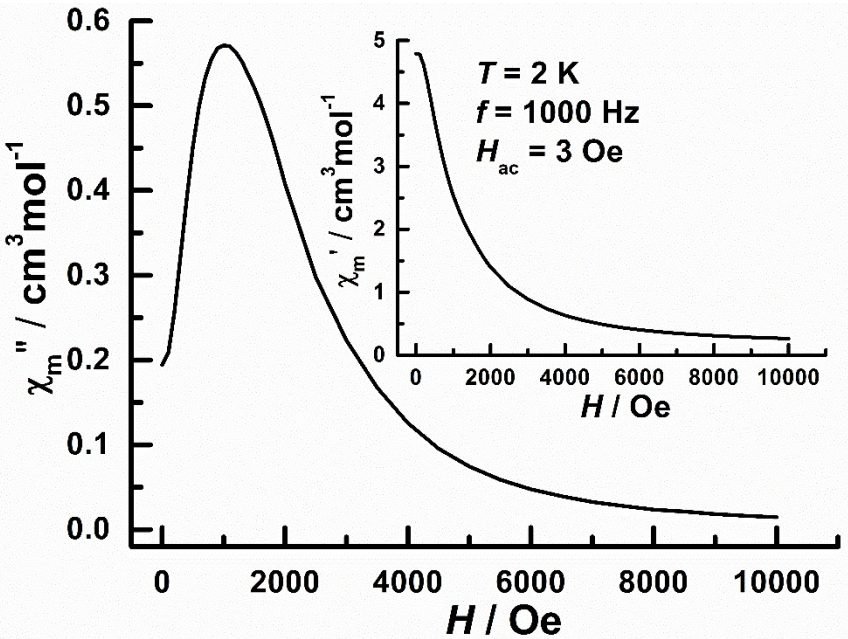

Fig. S6 Field dependence of the in-phase (χ', inset) and out-of-phase (χ'') ac susceptibility for **7** with f = 1000 Hz.

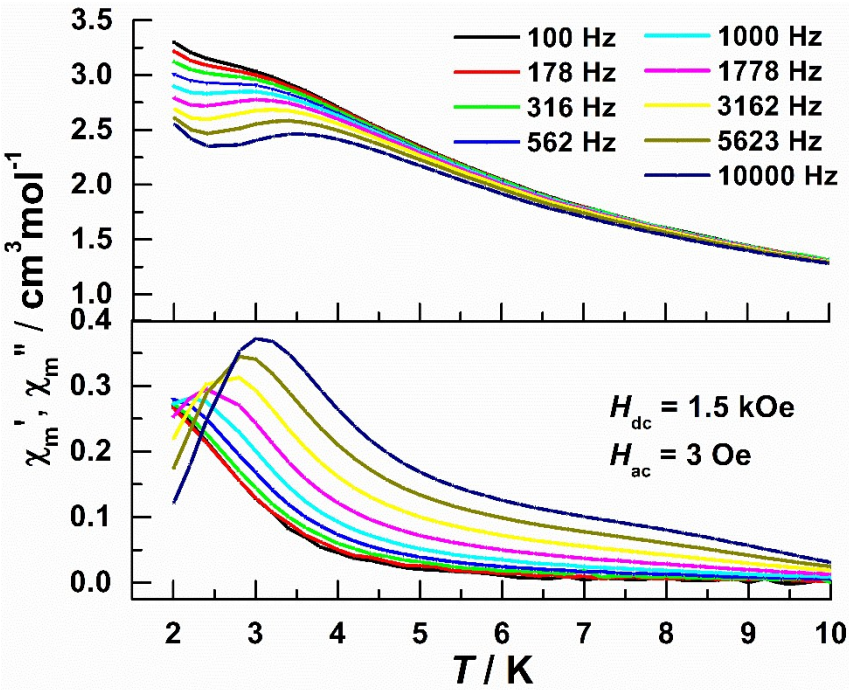

Fig. S7 Temperature dependence of χ' and χ'' ac susceptibility components under a 1.5 kOe dc field for **7**.

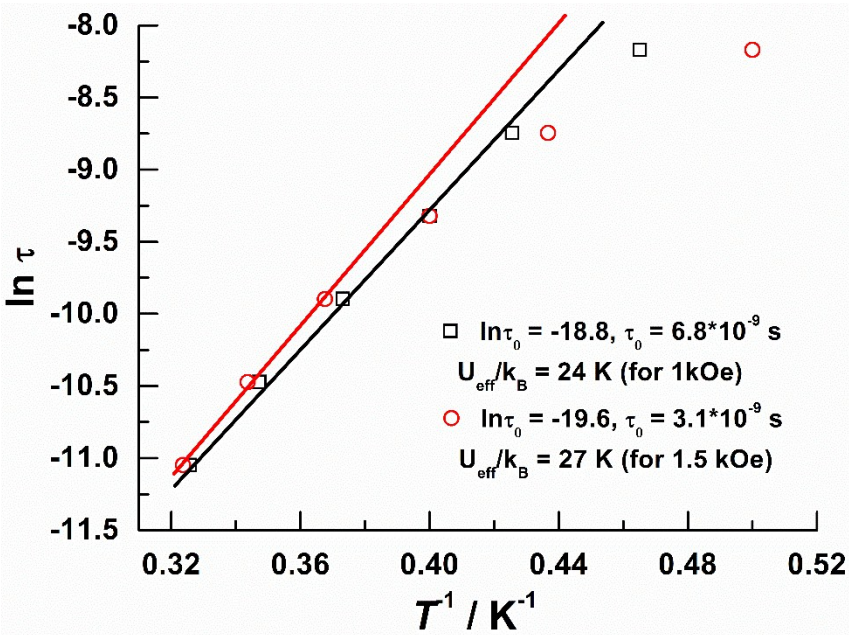

Fig. S8 Arrhenius analysis of **7** under a 1 and 1.5 kOe dc field.

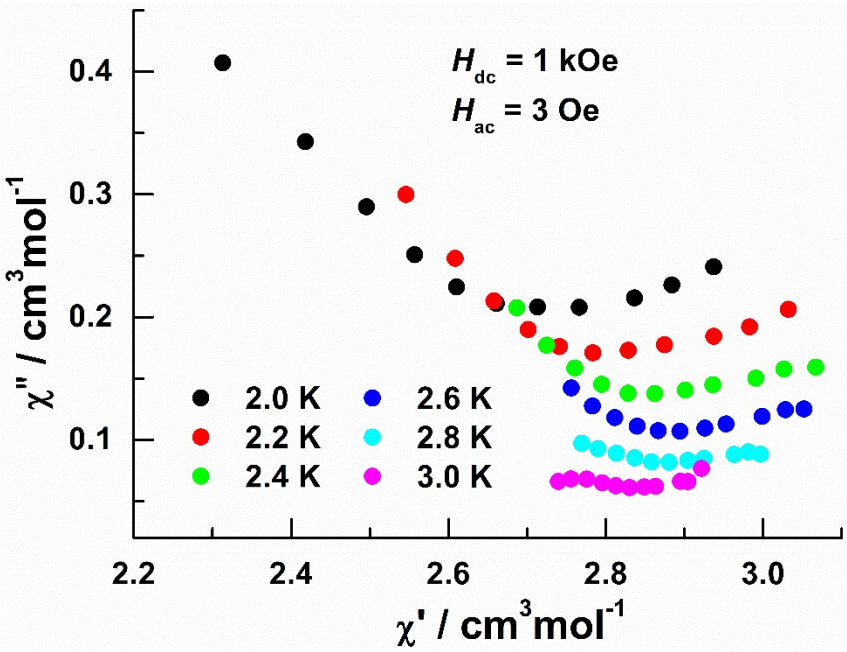

Fig. S9 The Cole–Cole plots of χ'' vs. χ' at 2.0, 2.2, 2.4, 2.6, 2.8 and 3.0 K for compound **1** under a 1 kOe dc field.

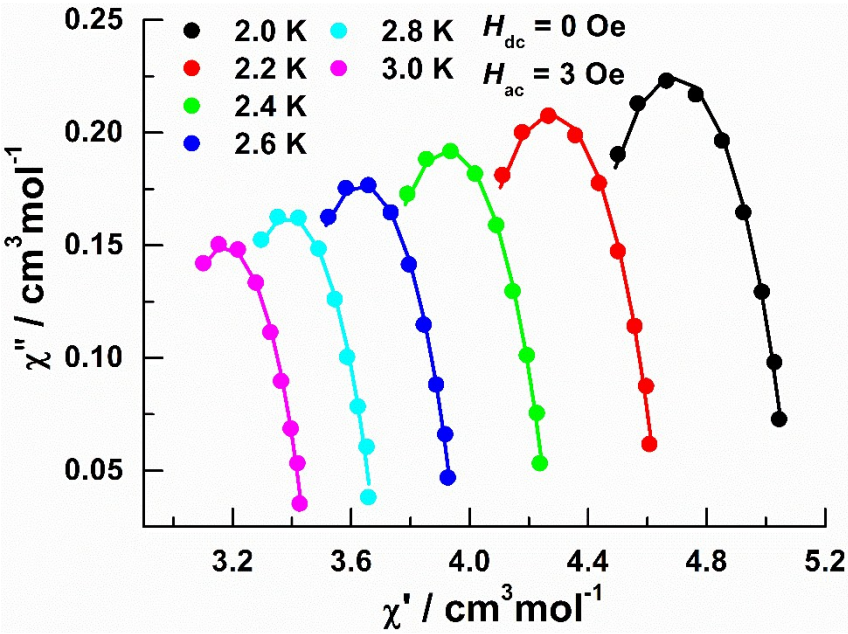

Fig. S10 The Cole–Cole plots of χ'' vs. χ' at 2.0, 2.2, 2.4, 2.6, 2.8 and 3.0 K for compound **7** under a zero dc field. The solid lines are the least-square fitting of the data to a distribution of single relaxation processes.

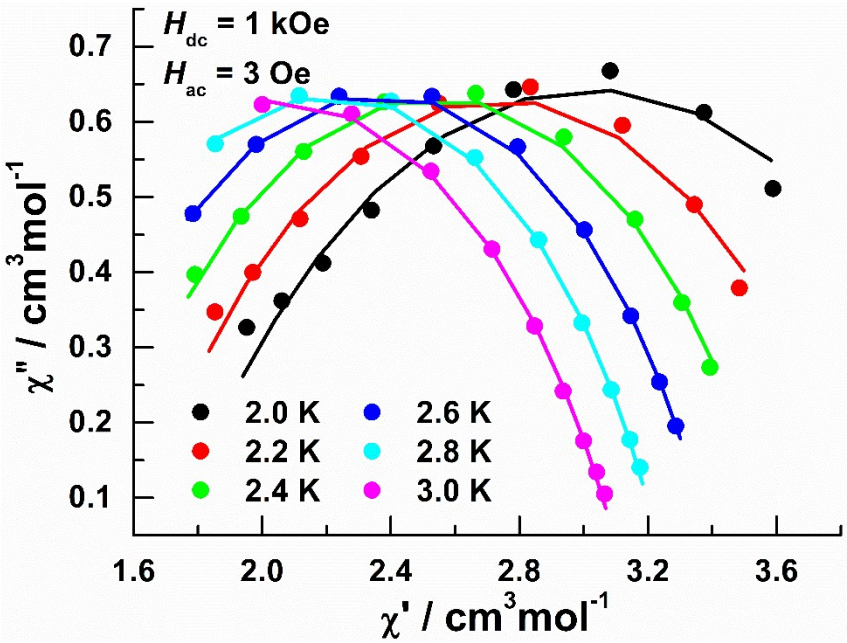

Fig. S11 The Cole–Cole plots of χ'' vs. χ' at 2.0, 2.2, 2.4, 2.6, 2.8 and 3.0 K for compound **7** under a 1 kOe dc field. The solid lines are the least-square fitting of the data to a distribution of single relaxation processes.

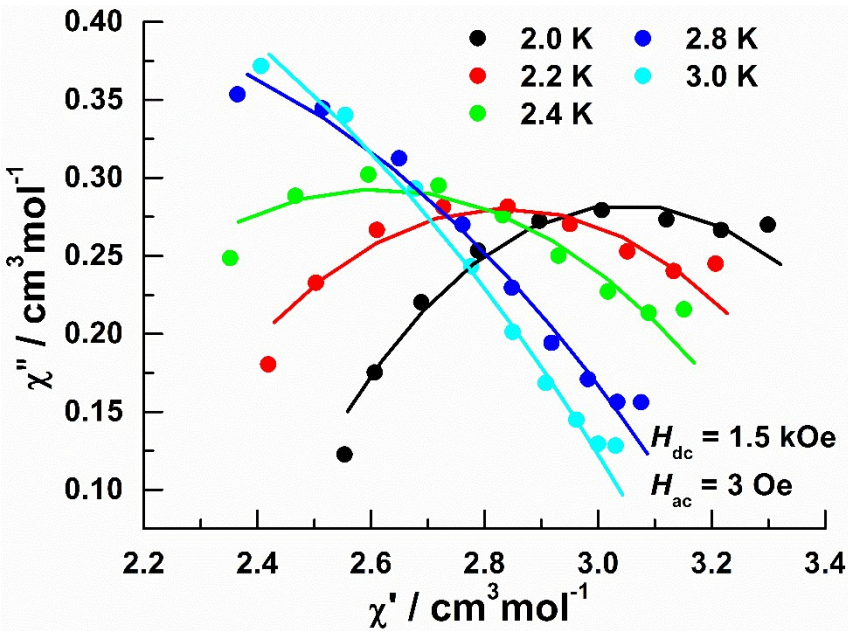

Fig. S12 The Cole–Cole plots of χ'' vs. χ' at 2.0, 2.2, 2.4, 2.8 and 3.0 K for compound **7** under a 1.5 kOe dc field. The solid lines are the least-square fitting of the data to a distribution of single relaxation processes.

Table S6 Relaxation parameters from the best fitting of the Cole–Cole diagrams by the generalized Debye model under a zero dc field for **7**.

T(K)	χ_S(cm^3 mol^{-1})	χ_T(cm^3 mol^{-1})	τ (s)	α
2.0	4.273	5.107	5.7×10^{-5}	0.37
2.2	3.889	4.662	5.2×10^{-5}	0.37
2.4	3.567	4.285	4.6×10^{-5}	0.37
2.6	3.303	3.968	4.1×10^{-5}	0.38
2.8	3.078	3.695	3.7×10^{-5}	0.38
3.0	2.889	3.459	3.3×10^{-5}	0.38

Table S7 Relaxation parameters from the best fitting of the Cole–Cole diagrams by the generalized Debye model under 1 kOe dc field for **7**.

T(K)	χ_S(cm^3 mol^{-1})	χ_T(cm^3 mol^{-1})	τ (s)	α
2.0	1.678	4.366	4.4×10^{-4}	0.43
2.2	1.576	3.899	2.2×10^{-4}	0.37
2.4	1.456	3.617	1.2×10^{-4}	0.33
2.6	1.327	3.414	6.5×10^{-5}	0.30
2.8	1.179	3.253	3.5×10^{-5}	0.30
3.0	0.949	3.123	1.7×10^{-5}	0.33

Table S8 Relaxation parameters from the best fitting of the Cole–Cole diagrams by the generalized Debye model under a 1.5 kOe dc field for **7**.

T(K)	χ_S(cm^3 mol^{-1})	χ_T(cm^3 mol^{-1})	τ (s)	α
2.0	2.363	3.739	3.8×10^{-4}	0.50
2.2	2.076	3.597	1.7×10^{-4}	0.55
2.4	1.738	3.485	5.6×10^{-5}	0.59
2.8	0.630	3.293	3.2×10^{-6}	0.63
3.0	0.000	3.191	1.1×10^{-6}	0.61